

PROBTS: A UNIFIED TOOLKIT TO PROBE DEEP TIME-SERIES FORECASTING

Jiawen Zhang^{1*}, Xumeng Wen², Shun Zheng², Jia Li¹, Jiang Bian²

¹HKUST(GZ) ²Microsoft Research Asia

jzhang302@connect.hkust-gz.edu.cn, jialeel@ust.hk
{xumengwen, shun.zheng, jiang.bian}@microsoft.com

ABSTRACT

Time-series forecasting serves as a linchpin in a myriad of applications, spanning various domains. With the growth of deep learning, this arena has bifurcated into two salient branches: one focuses on crafting specific neural architectures tailored for time series, and the other harnesses advanced deep generative models for probabilistic forecasting. While both branches have made significant progress, their differences across data scenarios, methodological focuses, and decoding schemes pose profound, yet unexplored, research questions. To bridge this knowledge chasm, we introduce `ProbTS`, a pioneering toolkit developed to synergize and compare these two distinct branches. Endowed with a unified data module, a modularized model module, and a comprehensive evaluator module, `ProbTS` allows us to revisit and benchmark leading methods from both branches. The scrutiny with `ProbTS` highlights their distinct characteristics, relative strengths and weaknesses, and areas that need further exploration. Our analyses point to new avenues for research, aiming for more effective time-series forecasting.¹

1 INTRODUCTION

Time-series forecasting serves as a cornerstone in many application scenarios across a plethora of domains, such as energy forecasting in solar applications (Rajagukguk et al., 2020), traffic prediction (Ghosh et al., 2009), climate projections (Angryk et al., 2020), and sustainable systems (Tai et al., 2023). Each scenario is unique, with distinct nuances in forecasting horizons, inherent temporal dependencies, and variations in data distributions.

With the meteoric rise of deep learning techniques in recent years (LeCun et al., 2015), deep time-series forecasting methods have increasingly gained traction. Diving deep into the existing methodologies, two salient research branches in this domain have emerged (Lim & Zohren, 2021). The first branch propelled by the groundbreaking success of customized neural network architectures in image and language domains, such as ResNets (He et al., 2016) and Transformer architectures (Vaswani et al., 2017). This branch focuses on crafting neural architectures tailored for time-series data representation (Oreshkin et al., 2020; Nie et al., 2023). On the other hand, the second branch is rooted in the advancements of deep generative models (Dinh et al., 2017; Papamakarios et al., 2017; Ho et al., 2020), looking to harness advanced probabilistic estimation methods for capturing intricate data distributions (Rasul et al., 2021b; Tashiro et al., 2021).

Given the diverse nature of time series forecasting tasks, these branches have pursued multiple avenues of innovation: from catering to different data characteristics and forecasting horizons to devising methodological focuses ranging from point forecasting via intricate neural architectures to probabilistic forecasting with nuanced density estimations. Furthermore, the branches exhibit distinct decoding schemes for multi-horizon forecasting, with the former majorly adopting non-autoregressive strategies and the latter inclining towards auto-regressive schemes.

Delving into the details, the first branch, with studies such as Zhou et al. (2021); Wu et al. (2021); Zhang et al. (2022); Challu et al. (2023); Nie et al. (2023), predominantly targets long-term forecast-

*This work was done during the internship at Microsoft Research Asia, Beijing, China.

¹This toolkit will be open-sourced.

ing, where data often reveals strong trends and seasonality patterns. Contrarily, the second branch, as showcased by works like (Salinas et al., 2019; Rasul et al., 2021b; Tashiro et al., 2021), is more oriented towards short-term forecasting, focusing on capturing detailed local variations and omitting significant trends or seasonality. Since different data characteristics and forecasting horizons may prefer widely different designs, this divergence naturally begs the question: how would the methodologies from one branch perform in scenarios traditionally addressed by the other?

From a methodological viewpoint, while the first branch specializes in neural network architecture design with inductive biases specifically for time-series data, they often restrict themselves to point forecasts. In contrast, the second branch, even with its keen interest in probabilistic forecasting, leans towards conventional neural network designs. The mystery then arises: what are the relative strengths and weaknesses of these two branches? And, can we integrate the strengths of both branches to revolutionize time-series forecasting?

Moreover, the decoding schemes chosen by these two branches exhibit a pronounced divergence. Methods in the first branch predominantly favor the non-autoregressive approach, projecting all future horizons in a single step. Whereas many methodologies in the second branch, illustrated by studies like (Salinas et al., 2019; Rasul et al., 2021b;a), adhere to the autoregressive scheme, generating forecasts step by step. This stark contrast between the two branches raises a compelling question: what underlying motivations and considerations steer this distinctive choice in decoding schemes? And, crucially, in the arena of time-series forecasting, which scheme showcases superior performance under diverse data scenarios?

Addressing these pressing research questions is paramount, as it can offer invaluable insights into the challenges and budding opportunities that come from harmonizing these two distinct research branches. Yet, despite the pressing need, there is an evident gap in the literature: no solution currently bridges the chasm between these branches, especially given the vast divergences in data scenarios, methodological focuses, and decoding schemes.

To enable comprehensive investigations on these inspiring research questions and to empower future research towards more effective time-series forecasting, this paper introduces `ProbTS`, an innovative toolkit tailored to unify and compare the research branch emphasizing neural architecture designs with the one focusing on advanced probabilistic estimations. At its core, `ProbTS` offers a unified *data* module, a modularized *model* module, and a holistic *evaluator* module. By harnessing `ProbTS`, we provide a comprehensive benchmark of some of the most pivotal methods from both branches, spanning a multitude of data scenarios and evaluation metrics. The outcomes of our analysis not only shed light on the previously stated research challenges but also unravel overlooked limitations in existing studies, charting the course for future time-series forecasting endeavors.

Contributions. We present `ProbTS`, a novel toolkit designed to bridge two distinct research branches in time-series forecasting, fostering in-depth analysis and comprehensive evaluation of leading methodologies across diverse scenarios and metrics. By utilizing `ProbTS`, we have summarized the following insights, shedding light on previously posed challenging questions:

- Regarding data scenarios, we find that long-term forecasting scenarios predominantly exhibit more significant trending and seasonality than short-term forecasting scenarios, while the latter typically display more complicated data distributions. These differences in data characteristics greatly influence the method designs of those two research branches.
- We have identified the pros and cons of different methodological focuses. Probabilistic forecasting methods indeed excel in modeling complex data distributions. However, we find that they may produce poor point forecasts even with superior CRPS scores. Additionally, customized network architectures, specifically addressing the challenges induced by trending and seasonality, perform remarkably well in long-term forecasting scenarios. Nevertheless, effective network architectures for short-term forecasting scenarios remain underexplored. These findings imply that there is a vast space to explore in future research, especially in combining these two research branches across various data scenarios.
- Concerning different decoding schemes, we find that the autoregressive scheme excels in cases with strong seasonality but struggles with pronounced trending, explaining why most long-term forecasting studies consistently prefer the non-autoregressive scheme. Furthermore, we observe that both decoding schemes perform equally well in short-term fore-

Table 1: Comparison of two research branches in time-series forecasting. Comparison dimensions include forecasting horizons, forecasting paradigms, architecture designs, and decoding schemes.

Model	Fore. Horizon		Fore. Paradigm		Arch. Design		Dec. Scheme	
	Short	Long	Point	Prob.	General	Customized	Auto.	Non-auto.
N-BEATS (Oreshkin et al., 2020)	✗	✓	✓	✗	✗	✓	✗	✓
Autoformer (Wu et al., 2021)	✗	✓	✓	✗	✗	✓	✗	✓
Informer (Zhou et al., 2021)	✗	✓	✓	✗	✗	✓	✗	✓
Pyraformer (Liu et al., 2022)	✗	✓	✓	✗	✗	✓	✗	✓
N-HiTS (Challu et al., 2023)	✗	✓	✓	✗	✗	✓	✗	✓
LTSF-Linear (Zeng et al., 2023)	✗	✓	✓	✗	✗	✓	✗	✓
PatchTST (Nie et al., 2023)	✗	✓	✓	✗	✗	✓	✗	✓
TimesNet (Wu et al., 2023)	✓	✓	✓	✗	✗	✓	✗	✓
DeepAR (Salinas et al., 2020)	✓	✗	✗	✓	✓	✗	✓	✗
GP-copula (Salinas et al., 2019)	✓	✗	✗	✓	✓	✗	✓	✗
LSTM NVP (Rasul et al., 2021b)	✓	✗	✗	✓	✓	✗	✓	✗
LSTM MAF (Rasul et al., 2021b)	✓	✗	✗	✓	✓	✗	✓	✗
Trans MAF (Rasul et al., 2021b)	✓	✗	✗	✓	✓	✗	✓	✗
TimeGrad (Rasul et al., 2021a)	✓	✗	✗	✓	✓	✗	✓	✗
CSDI (Tashiro et al., 2021)	✓	✗	✗	✓	✗	✓	✗	✓
SPD (Bilos et al., 2023)	✓	✗	✗	✓	✓	✗	✗	✓
ProbTS (Ours)	✓	✓	✓	✓	✓	✓	✓	✓

casting, which also explains the diverse preferences for these two schemes in short-term forecasting studies. Looking into the future, we also expect new autoregressive decoding schemes to address the error-propagation challenge when facing significant trending.

2 RELATED WORK

Time-series forecasting has witnessed significant advancements in recent years, giving rise to two distinct research branches: one focused on effective network architecture designs, and the other dedicated to advancing probabilistic estimation. In Table 1, we present representative studies from these two branches and compare them with ProbTS across various aspects. In the following, we provide a comprehensive review of these two branches and discuss existing time-series forecasting toolkits, highlighting the unique features of ProbTS.

Neural Architecture Designs in Time-series Forecasting. A substantial body of research has been dedicated to enhancing neural architecture designs for time-series forecasting. Notable examples include extensions of multi-layer perceptrons (Oreshkin et al., 2020; Fan et al., 2022; Zhang et al., 2022; Challu et al., 2023; Zeng et al., 2023; Ekambaram et al., 2023), customized recurrent or convolutional neural networks (Lai et al., 2018; LIU et al., 2022; Wu et al., 2023), and more recently, various Transformer-based variants developed (Vaswani et al., 2017; Li et al., 2019; Zhou et al., 2021; Wu et al., 2021; Zhou et al., 2022; Liu et al., 2022; Zhang & Yan, 2022; Cirstea et al., 2022; Nie et al., 2023). One common characteristic of studies in this branch is their typical use of the non-autoregressive decoding scheme, projecting into future horizons at once. Moreover, a significant portion of these studies, especially recent Transformer variants, primarily focuses on evaluating long-term forecasting scenarios, often characterized by prominent trending and seasonality patterns. Despite their advancements in neural architecture designs, these studies often limit themselves to point forecasts, capturing only the average variations of future values rather than the underlying data distribution. While approaches like quantile regression (Wen et al., 2017; Lim et al., 2021) can mitigate this limitation, they cannot replace the inherent capture of the data distribution.

Probabilistic Estimation in Time-series Forecasting. In contrast to the first branch, which predominantly considers point forecasts, the second branch, commonly referred to as *deep probabilistic time-series forecasting*, aims to leverage deep neural networks to capture the complex data distribu-

tion of future time series. This branch has garnered broad research attention, ranging from early approaches employing pre-defined likelihood functions (Rangapuram et al., 2018; Salinas et al., 2020) or Gaussian copulas (Salinas et al., 2019; Drouin et al., 2022) to more recent methods harnessing advanced deep generative models (Rasul et al., 2021b;a; Tashiro et al., 2021; Bilos et al., 2023). While studies in this branch can produce probabilistic forecasts, including distributional information about future time-series variations, they primarily evaluate short-term forecasting scenarios, inevitably overlooking the challenges posed by long-term trending or seasonality. A noteworthy observation is that, unlike studies in the first branch, which consistently prefer the non-autoregressive scheme, studies in this branch have employed both autoregressive (Rasul et al., 2021b;a) and non-autoregressive (Tashiro et al., 2021; Li et al., 2022) decoding schemes. Furthermore, in contrast to the flourishing development of specific neural architecture designs in the first branch, this research focus is relatively underexplored in the second branch. While a few methods (Tashiro et al., 2021; Li et al., 2022; Bergsma et al., 2022) incorporate customized neural architectures, more studies (de Bézenac et al., 2020; Rasul et al., 2021b;a; Bilos et al., 2023; Drouin et al., 2022) leverage standardized neural architectures to encode time-series representations.

Time-series Forecasting Toolkits. Parallel to the divergence of time-series research into two branches, we have also witnessed the emergence of two types of toolkits for time-series forecasting. The first type, primarily oriented towards point forecasting, includes Prophet (Taylor & Letham, 2018), sktime (Löning et al., 2019), tsai (Oguiza, 2022), TSlib (Wu et al., 2023), as well as other open-source implementations of studies from the first research branch. The second type, emphasizing probabilistic forecasting, encompasses GluonTS (Alexandrov et al., 2020) and PyTorchTS (Rasul et al., 2021b). However, these two types of toolkits, each specializing in a single forecasting paradigm, fall short of our research objective to unify the two distinct research branches. Two exceptions to this are PyTorchForecasting² and NeuralForecast³, both of which incorporate customized neural architectures and probabilistic forecasters. Although these two toolkits come close to our work, they only cover a limited range of approaches, notably lacking more advanced probabilistic forecasting methods (Rasul et al., 2021b;a; Tashiro et al., 2021), and their pipelines are ill-suited for direct investigations into our research questions of interest. In contrast, `PROBTS` is purpose-built to unify and compare the latest research in neural architecture designs with cutting-edge studies in probabilistic forecasting. Most importantly, `PROBTS` aims to uncover overlooked limitations in existing approaches and identify new opportunities for future research to enhance the effectiveness of time-series forecasting.

3 THE `PROBTS` TOOLKIT

This section starts with a formal description of time series forecasting, then elaborates on three pivotal modules, including a unified *data* module to manage varying data scenarios, a modularized *model* module to accommodate diverse methodological approaches and decoding schemes, and a holistic *evaluator* for an all-encompassing assessment.

Problem Formulation. Formally, we denote an element of a multivariate time series as $x_t^k \in \mathbb{R}$, where k represents the variate index and t denotes the time index. At time step t , we have a multivariate vector $\mathbf{x}_t \in \mathbb{R}^K$. Each x_t^k is associated with covariates $\mathbf{c}_t^k \in \mathbb{R}^N$, which encapsulates auxiliary information about the observations. Given a length- T forecast horizon a length- L observation history $\mathbf{x}_{t-L:t}$ and corresponding covariates $\mathbf{c}_{t-L:t}$, the objective in time series forecasting is to generate the vector of future values $\mathbf{x}_{t+1:t+T}$. In `PROBTS`, we decouple a model into an encoder f_ϕ and a forecaster p_θ . An encoder is tasked with generating expressive hidden states $\mathbf{h} \in \mathbb{R}^D$. Under *autoregressive* decoding scheme, encoder forecasts variates using their past values, which can be formulated as $\mathbf{h}_t = f_\phi(\mathbf{x}_{t-1}, \mathbf{c}_t, \mathbf{h}_{t-1})$. Under the *non-autoregressive* scheme, the encoder generates all the forecasts in one step, which can be expressed as $\mathbf{h}_{t+1:t+T} = f_\phi(\mathbf{x}_{t-L:t}, \mathbf{c}_{t-L:t+T})$. A forecaster p_θ is employed either to directly estimate *point forecasts* as $\hat{\mathbf{x}}_t = p_\theta(\mathbf{h}_t)$, or to perform sampling based on the estimated *probabilistic distributions* as $\hat{\mathbf{x}}_t \sim p_\theta(\mathbf{x}_t | \mathbf{h}_t)$.

²<https://github.com/jdb78/pytorch-forecasting>

³<https://github.com/Nixtla/neuralforecast>

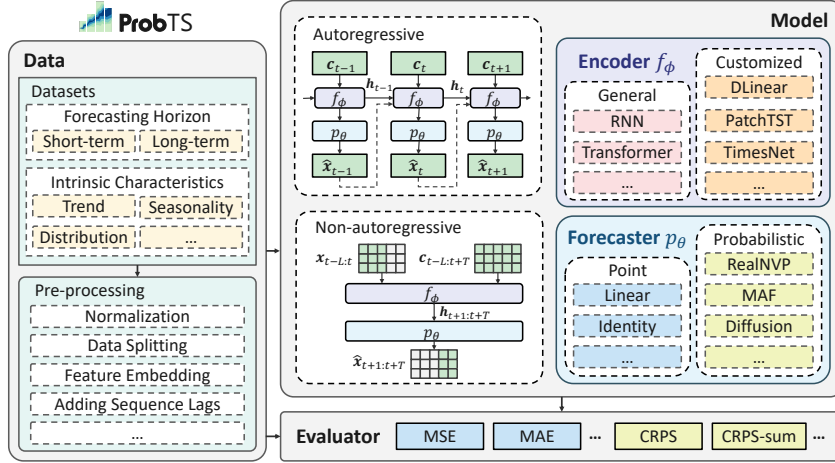


Figure 1: An overview of ProBTs.

Data. The data module unifies varied data scenarios to facilitate thorough evaluation and implements standardized pre-processing techniques to ensure fair comparison. Moreover, we utilize a quantitative approach to visually delineate datasets’ intrinsic characteristics, which employs decomposition to assess trends and seasonality in a time series and evaluate the similarity between data distribution and a Gaussian to depict the complexity of data distribution. Descriptions and statistics for each dataset are listed in Table 2, and a quantitative evaluation of their inherent properties is provided in Table 3. We attach the detailed quantitative calculation process in Appendix A.

Model. The modularized model module accommodates diverse neural network architectures, forecasting paradigms, and decoding schemes. Adhering to the decoupled model formulation from Section 3, it enables the construction of various models by configuring the encoder f_ϕ and forecaster p_θ . For example, point estimation methods like DLinear centralize their design in the encoder, using a linear layer or identity mapping as the forecaster, with non-autoregressive decoding. In contrast, probabilistic models like TimeGrad incorporate general neural architectures in the encoder and advanced probabilistic techniques in the forecaster, employing autoregressive decoding.

Evaluator. The evaluator module integrates a diverse array of evaluation metrics such as Mean Absolute Error (MAE), Normalized Mean Absolute Error (NMAE), Mean Square Error (MSE), and Continuous Ranked Probability Score (CRPS), allowing for assessment of both point-level and distribution-level accuracies. We employ the NMAE metric for point-level evaluation to accommodate different scales of errors, and unlike previous studies (Rasul et al., 2021a; Tashiro et al., 2021) that used the CRPS_{sum} metric, we utilize CRPS for our analysis for a refined evaluation of each variate’s probability distribution accuracy. A detailed list of evaluation metrics and their formal definitions can be found in Appendix B.

Implementation. To ensure the integrity of the results, ProBTs adheres to a standard implementation process, employing unified data splitting, standardization techniques, and adopting fair settings for hyperparameter tuning across all methods. We utilize reported optimal hyperparameters for models directly associated with specific datasets and conduct an extensive grid search to identify the most effective settings for those hyperparameters that were not available. Details regarding the experimental setup can be found in Appendix C.

4 PROBE DEEP TIME SERIES FORECASTING

In this section, our analysis is started by discussing variations in data scenarios (Section 4.1), and then we evaluate the strengths and weaknesses of different methodological focuses (Sections 4.2 and 4.3) and decoding schemes (Section 4.4). Finally, we compare the computational efficiencies of these approaches in Section 4.5.

Table 2: Dataset Summary.

Horizon	Dataset	#var.	range	freq.	timesteps	Description
Long-term	ETTh1/h2	7	\mathbb{R}^+	H	17,420	Electricity transformer temperature per hour
	ETTh1/m2	7	\mathbb{R}^+	15min	69,680	Electricity transformer temperature every 15 min
	Electricity	321	\mathbb{R}^+	H	26,304	Electricity consumption (Kwh)
	Traffic	862	(0,1)	H	17,544	Road occupancy rates
	Exchange	8	\mathbb{R}^+	Busi. Day	7,588	Daily exchange rates of 8 countries
	ILI	7	(0,1)	W	966	Ratio of patients seen with influenza-like illness
	Weather	21	\mathbb{R}^+	10min	52,696	Local climatological data
Short-term	Exchange	8	\mathbb{R}^+	Busi. Day	6,071	Daily exchange rates of 8 countries
	Solar	137	\mathbb{R}^+	H	7,009	Solar power production records
	Electricity	370	\mathbb{R}^+	H	5,833	Electricity consumption
	Traffic	963	(0,1)	H	4,001	Road occupancy rates
	Wikipedia	2,000	\mathbb{N}	D	792	Page views of 2000 Wikipedia pages

Baseline selection. For probabilistic approaches, we incorporate models utilizing advanced density estimation techniques such as normalizing flows (GRU NVP, GRU MAF, and Trans MAF) and diffusion models (TimeGrad and CSDI). To investigate the influence of probabilistic modeling, we also consider general neural network architectures like Linear, GRU, and Transformer, coupled with a linear forecaster without probabilistic estimation. Global mean and batch mean are integrated as baselines to assess forecasting difficulty. In addition, we include TimesNet and PatchTST, leading approaches in models with architectures refined for time series, and N-HiTS and LTSE-Linear (NLinear and DLinear), distinguished by their unique designs for modeling time series data.

Table 3: Quantitative assessment of intrinsic characteristics for each dataset. To eliminate ambiguity, we use the suffix "-S" and "-L" to denote short-term and long-term forecasting datasets, respectively. The JS Div denotes Jensen–Shannon divergence, where a lower score indicates closer approximations to a Gaussian distribution.

Dataset	Exchange-S	Solar-S	Electricity-S	Traffic-S	Wikipedia-S	ETTh1-L	ETTh2-L
Trend F_T	0.9982	0.1688	0.6443	0.2880	0.5253	0.9462	0.9770
Seasonality F_S	0.1256	0.8592	0.8323	0.6656	0.2234	0.0105	0.0612
JS Div.	0.2967	0.5004	0.3579	0.2991	0.2751	0.0833	0.1701
Dataset	ETTh1-L	ETTh2-L	Electricity-L	Traffic-L	Weather-L	Exchange-L	ILI-L
Trend F_T	0.7728	0.9412	0.6476	0.1632	0.9612	0.9978	0.5438
Seasonality F_S	0.4772	0.3608	0.8344	0.6798	0.2657	0.1349	0.6075
JS Div.	0.0719	0.1422	0.1533	0.1378	0.1727	0.1082	0.1112

4.1 DATASET SCENARIOS

By unifying data scenarios, we can ascertain how existing methods perform on previously unevaluated data scenarios. This enables a deeper understanding of the motivations behind distinct designs, which are usually influenced by varied data characteristics.

Differences in data characteristics. Table 3 reveals that certain datasets, such as Exchange and ETT, exhibit robust trends with limited seasonality. On the other hand, datasets such as Solar and Traffic display reduced trendiness but substantial seasonality dominance. These variations impose distinct demands on a model’s ability to handle trends and seasonality effectively. Moreover, the table illustrates the considerable divergences in data distributions among datasets. Typically, datasets closely adhering to a Gaussian distribution, such as Wikipedia-S, do not require much distribution modeling capabilities. Whereas datasets that deviate from the Gaussian distribution, e.g., Solar-S and Electricity-S, necessitate more advanced distribution modeling designs.

Impacts of forecasting horizons. To gain intuitive insights, we present visualizations of time series instances in Appendix A. Figure 2 and Figure 3 visually convey the impacts of varying forecasting horizons, showcasing instances of time series for short-term and long-term datasets respectively.

Table 4: Results (mean_{std}) on short-term forecasting datasets. We obtain mean and standard error metrics by re-training and evaluating five times.

Model	Exchange Rate		Solar		Electricity		Traffic		Wikipedia	
	CRPS	NMAE	CRPS	NMAE	CRPS	NMAE	CRPS	NMAE	CRPS	NMAE
Glob. mean	0.188	0.188	1.403	1.403	0.412	0.412	0.540	0.540	0.577	0.577
Batch mean	0.012	0.012	1.244	1.244	0.365	0.365	0.503	0.503	0.336	0.336
Linear	0.012 _{.001}	0.012 _{.001}	0.704 _{.036}	0.704 _{.036}	0.138 _{.009}	0.138 _{.009}	0.327 _{.032}	0.327 _{.032}	0.874 _{.151}	0.874 _{.151}
GRU	0.013 _{.002}	0.013 _{.002}	0.594 _{.144}	0.594 _{.144}	0.134 _{.009}	0.134 _{.009}	0.193 _{.002}	0.193 _{.002}	0.394 _{.013}	0.394 _{.013}
Transformer	0.016 _{.001}	0.016 _{.001}	0.538 _{.066}	0.538 _{.066}	0.115 _{.005}	0.115 _{.005}	0.204 _{.006}	0.204 _{.006}	0.408 _{.011}	0.408 _{.011}
N-HiTS	0.012 _{.000}	0.012 _{.000}	0.572 _{.020}	0.572 _{.020}	0.074 _{.003}	0.074 _{.003}	0.193 _{.002}	0.193 _{.002}	0.332 _{.011}	0.332 _{.011}
NLinear	0.010 _{.000}	0.010_{.000}	0.560 _{.002}	0.560 _{.002}	0.083 _{.002}	0.083 _{.002}	0.233 _{.001}	0.233 _{.001}	0.321 _{.001}	0.321 _{.001}
DLinear	0.012 _{.001}	0.012 _{.001}	0.547 _{.009}	0.547 _{.009}	0.095 _{.006}	0.095 _{.006}	0.273 _{.012}	0.273 _{.012}	1.046 _{.037}	1.046 _{.037}
PatchTST	0.010 _{.000}	0.010_{.000}	0.496 _{.002}	0.496 _{.002}	0.076 _{.001}	0.076 _{.001}	0.202 _{.001}	0.202 _{.001}	<u>0.257_{.001}</u>	0.257_{.001}
TimesNet	0.011 _{.001}	0.011 _{.001}	0.507 _{.019}	0.507 _{.019}	0.071 _{.002}	0.071 _{.002}	0.205 _{.002}	0.205 _{.002}	0.304 _{.002}	0.304 _{.002}
GRU NVP	0.016 _{.003}	0.020 _{.003}	0.396 _{.021}	0.507 _{.022}	0.055 _{.002}	0.073 _{.003}	0.161 _{.006}	0.203 _{.009}	0.282 _{.003}	0.330 _{.003}
GRU MAF	0.015 _{.001}	0.020 _{.001}	0.386 _{.026}	0.492 _{.027}	0.051 _{.001}	0.067 _{.001}	0.131 _{.006}	0.165 _{.009}	0.281 _{.004}	0.337 _{.005}
Trans MAF	0.011 _{.001}	0.014 _{.001}	0.400 _{.022}	0.503 _{.022}	0.054 _{.004}	0.071 _{.005}	0.129_{.004}	0.165_{.006}	0.289 _{.008}	0.344 _{.008}
TimeGrad	0.011 _{.001}	0.014 _{.002}	0.359_{.011}	0.445_{.023}	0.052 _{.001}	0.067 _{.001}	0.164 _{.091}	0.201 _{.115}	0.272 _{.008}	0.327 _{.011}
CSDI	0.008_{.000}	0.011 _{.000}	0.366 _{.005}	0.484 _{.008}	0.050_{.001}	0.065_{.001}	0.146 _{.012}	0.176 _{.013}	0.219_{.006}	0.259 _{.009}

Table 5: Results (mean_{std}) on long-term forecasting datasets. The input sequence length is set to 36 for the ILI dataset and 96 for the others. We obtain mean and standard error metrics by re-training and evaluating three times. Due to the excessive time consumption of CSDI in high-dimensional scenarios, results are unavailable in partial long-term forecasting datasets.

Model	pred len	DLinear		PatchTST		GRU NVP		TimeGrad		CSDI	
		CRPS	NMAE	CRPS	NMAE	CRPS	NMAE	CRPS	NMAE	CRPS	NMAE
ETTh1	96	0.282 _{.002}	0.282 _{.002}	0.272 _{.001}	0.272 _{.001}	0.383 _{.053}	0.488 _{.058}	0.522 _{.105}	0.645 _{.129}	0.236_{.006}	0.308 _{.005}
	192	0.309 _{.004}	0.309 _{.004}	0.295 _{.001}	0.295 _{.001}	0.396 _{.030}	0.514 _{.042}	0.603 _{.092}	0.748 _{.084}	0.291_{.025}	0.377 _{.026}
	336	0.338 _{.008}	0.338 _{.008}	0.323 _{.001}	0.323 _{.001}	0.486 _{.032}	0.630 _{.029}	0.601 _{.028}	0.759 _{.015}	0.322_{.033}	0.419 _{.042}
	720	0.387 _{.029}	0.387 _{.029}	0.353_{.001}	0.353_{.001}	0.546 _{.036}	0.707 _{.050}	0.621 _{.037}	0.793 _{.034}	0.448 _{.038}	0.578 _{.051}
ETTh2	96	0.138 _{.000}	0.138 _{.000}	0.132 _{.001}	0.132 _{.001}	0.319 _{.044}	0.413 _{.059}	0.427 _{.042}	0.525 _{.047}	0.115_{.009}	0.146 _{.012}
	192	0.163 _{.003}	0.163 _{.003}	0.157 _{.001}	0.157 _{.001}	0.326 _{.025}	0.427 _{.033}	0.424 _{.061}	0.530 _{.060}	0.147_{.008}	0.189 _{.012}
	336	0.188 _{.001}	0.188 _{.001}	0.176_{.000}	0.176_{.000}	0.449 _{.145}	0.580 _{.169}	0.469 _{.049}	0.566 _{.047}	0.190 _{.018}	0.248 _{.024}
	720	0.219 _{.003}	0.219 _{.003}	0.205_{.001}	0.205_{.001}	0.561 _{.273}	0.749 _{.385}	0.470 _{.054}	0.561 _{.044}	0.239 _{.035}	0.306 _{.040}
ETTh1	96	0.352 _{.011}	0.352 _{.011}	0.328_{.003}	0.328_{.003}	0.379 _{.030}	0.481 _{.037}	0.455 _{.046}	0.585 _{.058}	0.437 _{.018}	0.557 _{.022}
	192	0.393 _{.001}	0.393 _{.001}	0.359_{.002}	0.359_{.002}	0.425 _{.019}	0.531 _{.018}	0.516 _{.038}	0.680 _{.058}	0.496 _{.051}	0.625 _{.065}
	336	0.419 _{.007}	0.419 _{.007}	0.384_{.002}	0.384_{.002}	0.458 _{.054}	0.580 _{.064}	0.512 _{.026}	0.666 _{.047}	0.454 _{.025}	0.574 _{.026}
	720	0.502 _{.029}	0.502 _{.029}	0.397_{.002}	0.397_{.002}	0.502 _{.039}	0.643 _{.046}	0.523 _{.027}	0.672 _{.015}	0.528 _{.012}	0.657 _{.014}
ETTh2	96	0.211 _{.027}	0.211 _{.027}	0.177 _{.000}	0.177 _{.000}	0.432 _{.141}	0.548 _{.158}	0.358 _{.026}	0.448 _{.031}	0.164_{.013}	0.214 _{.018}
	192	0.238 _{.028}	0.238 _{.028}	0.201_{.001}	0.201_{.001}	0.625 _{.170}	0.766 _{.223}	0.457 _{.081}	0.575 _{.089}	<u>0.226_{.018}</u>	0.294 _{.027}
	336	0.284 _{.008}	0.284 _{.008}	0.240_{.001}	0.240_{.001}	0.793 _{.319}	0.942 _{.408}	0.481 _{.078}	0.606 _{.095}	<u>0.274_{.022}</u>	0.353 _{.028}
	720	0.307 _{.000}	0.307 _{.000}	0.252_{.000}	0.252_{.000}	0.539 _{.090}	0.688 _{.161}	0.445 _{.016}	0.550 _{.018}	<u>0.302_{.040}</u>	0.382 _{.030}
Electricity	96	0.090 _{.001}	0.090 _{.001}	0.086_{.001}	0.086_{.001}	0.094 _{.003}	0.118 _{.003}	0.096 _{.002}	0.119 _{.003}	0.153 _{.137}	0.203 _{.189}
	192	0.095 _{.001}	0.095 _{.001}	0.092_{.001}	0.092_{.001}	0.097 _{.002}	0.121 _{.003}	0.100 _{.004}	0.124 _{.005}	0.200 _{.094}	0.264 _{.129}
	336	0.104 _{.000}	0.104 _{.000}	0.100 _{.000}	0.100 _{.000}	0.099_{.001}	0.123 _{.001}	0.102 _{.007}	0.126 _{.008}	-	-
	720	0.122 _{.001}	0.122 _{.001}	0.116 _{.000}	0.116 _{.000}	0.114 _{.013}	0.144 _{.017}	0.108_{.003}	0.134 _{.004}	-	-
Traffic	96	0.356 _{.009}	0.356 _{.009}	0.248 _{.001}	0.248 _{.001}	0.187_{.002}	0.231_{.003}	0.202 _{.004}	0.234 _{.006}	-	-
	192	0.346 _{.009}	0.346 _{.009}	0.245 _{.001}	0.245 _{.001}	0.192_{.001}	0.236_{.002}	0.208 _{.003}	0.239 _{.004}	-	-
	336	0.350 _{.008}	0.350 _{.008}	0.257 _{.002}	0.257 _{.002}	0.201_{.004}	0.248_{.006}	0.213 _{.003}	0.246_{.003}	-	-
	720	0.365 _{.009}	0.365 _{.009}	0.266 _{.001}	0.266 _{.001}	0.211_{.004}	0.264_{.006}	0.220 _{.002}	0.263_{.001}	-	-
Weather	96	0.112 _{.001}	0.112 _{.001}	0.087 _{.002}	0.087 _{.002}	0.116 _{.013}	0.145 _{.017}	0.130 _{.017}	0.164 _{.023}	0.068_{.008}	0.087 _{.012}
	192	0.122 _{.001}	0.122 _{.001}	0.090 _{.001}	0.090 _{.001}	0.122 _{.021}	0.147 _{.025}	0.127 _{.019}	0.158 _{.024}	0.068_{.006}	0.086_{.007}
	336	0.130 _{.002}	0.130 _{.002}	0.092 _{.002}	0.092 _{.002}	0.128 _{.011}	0.160 _{.012}	0.130 _{.006}	0.162 _{.006}	0.083_{.002}	0.098 _{.002}
	720	0.144 _{.001}	0.144 _{.001}	0.094 _{.001}	0.094 _{.001}	0.110 _{.004}	0.135 _{.008}	0.113 _{.011}	0.136 _{.020}	0.087_{.003}	0.102 _{.005}
Exchange	96	0.024 _{.000}	0.024 _{.000}	0.023_{.000}	0.023_{.000}	0.071 _{.006}	0.091 _{.009}	0.068 _{.003}	0.079 _{.002}	0.028 _{.003}	0.036 _{.005}
	192	0.035 _{.000}	0.035 _{.000}	0.034_{.000}	0.034_{.000}	0.068 _{.004}	0.087 _{.005}	0.087 _{.013}	0.100 _{.019}	0.045 _{.003}	0.058 _{.005}
	336	0.048 _{.001}	0.048 _{.001}	0.048_{.000}	0.048_{.000}	0.072 _{.002}	0.091 _{.002}	0.074 _{.009}	0.086 _{.008}	0.060 _{.004}	0.076 _{.006}
	720	0.075 _{.002}	0.075 _{.002}	0.072_{.000}	0.072_{.000}	0.079 _{.009}	0.103 _{.009}	0.099 _{.015}	0.113 _{.016}	0.143 _{.020}	0.173 _{.020}
ILI	24	0.213 _{.038}	0.213 _{.038}	0.169_{.005}	0.169_{.005}	0.257 _{.003}	0.283 _{.001}	0.275 _{.047}	0.296 _{.044}	0.250 _{.013}	0.263 _{.012}
	36	0.230 _{.015}	0.230 _{.015}	0.156_{.005}	0.156_{.005}	0.281 _{.004}	0.307 _{.007}	0.272 _{.057}	0.298 _{.048}	0.285 _{.010}	0.285 _{.011}
	48	0.221 _{.009}	0.221 _{.009}	0.156_{.008}	0.156_{.008}	0.288 _{.008}	0.314 _{.009}	0.295 _{.033}	0.320 _{.025}	0.285 _{.036}	0.301 _{.034}
	60	0.230 _{.013}	0.230 _{.013}	0.147_{.003}	0.147_{.003}	0.307 _{.005}	0.333 _{.005}	0.295 _{.083}	0.325 _{.068}	0.283 _{.012}	0.299 _{.013}

Figure 2 emphasizes that short-term contexts are primarily characterized by local variations. Conversely, Figure 3 demonstrates an augmented presence of seasonality and trends in datasets like Traffic, Electricity, and ETT under elongated forecasting horizons, enhancing predictability. This

shift highlights the importance of capturing local dynamics in short-term forecasting, while longer forecasting horizons necessitate models adept at modeling extended seasonality and trends.

4.2 POINT VS. PROBABILISTIC ESTIMATION

Beyond differing data scenarios, varied methodological focuses raise essential questions about the unique benefits of specialized model designs, especially probabilistic estimation.

Probabilistic methods excel in modeling complex data distributions. From Table 4, it is evident that probabilistic estimation methods, especially TimeGrad and CSDI, demonstrate superior performance in both NMAE and CRPS metrics in short-term forecasting. This advantage is particularly notable in the Solar, Electricity, and Traffic datasets, which show intricate data distributions in Table 3. This underscores the aptitude of probabilistic methods in addressing complex data distributions. Whereas for long-term forecasts, we cannot compare probabilistic and point estimation methods solely based on data distribution since the performance is multifacetedly affected.

Probabilistic methods may produce poor point forecasts even with a superior CRPS score. Table 5 illustrates that while probabilistic methods like CSDI demonstrate prowess in the CRPS metric, they lag in NMAE, reflecting precise distribution approximations but weaker point forecasts. This discrepancy is indicative of inherent limitations in current probabilistic models, shedding light on the prevailing preference for CRPS in evaluations. It highlights substantial opportunities for refining probabilistic approaches and underscores the critical need for holistic evaluation perspectives to enhance the reliability and precision of time-series forecasting.

The complex local variations inherent to shorter forecasting horizons, as detailed in Section 4.1, explain why most probabilistic forecasting studies opt for short-term datasets for model evaluation. However, proficiency in one aspect is insufficient in real-world applications, and the ability to handle other intrinsic data characteristics is equally crucial, which calls for a more comprehensive evaluation setting.

4.3 CUSTOMIZED VS. GENERAL NEURAL ARCHITECTURE

In addition to exploring the advantages of probabilistic estimation, the pressing question of whether a customized neural architecture with time-series inductive bias is essential remains unresolved.

Customized network architecture performs remarkably on long-term forecasting. Table 5 illustrates that in long-term forecasting, models with time-series inductive bias like DLinear and PatchTST significantly outperform models that employ advanced probabilistic estimation techniques but rely solely on general architectures. Given that data exhibit more pronounced seasonality and trends in longer forecast horizons, as discussed in Section 4.1, we attribute this superiority to their trend-seasonality decomposition techniques. This suggests that a general architecture is not enough for time-series modeling, and incorporating more unique designs tailored for time-series domain knowledge is expected.

Customized network architecture on short-term forecasting remains underexplored. Different from long-term forecasting, Table 4 suggests short-term forecasting does not significantly benefit from existing customized network architectures compared to general ones. Exceptions like the Exchange and Wikipedia datasets are influenced by their intrinsic characteristics; the former is smooth, allowing even basic models like batch mean to succeed (see Table 4.1), while the latter includes abundant outliers pose challenges for all models (see Table 7). Thus, the development and refinement of network architectures to better apprehend short-term fluctuations represent a pivotal and unmet challenge.

Our findings expose the performance gap of distinct designs across diverse data scenarios, explaining the preference of different methodological focuses for unique dataset settings. This insight uncovers a potential path to revolutionize time-series forecasting by harnessing the strengths of both neural network architectures with time-series inductive bias and probabilistic estimation methods. Such an amalgamation enables effective modeling of intricate data distributions while adeptly managing the inherent periodicity and seasonality of time series.

4.4 AUTOREGRESSIVE VS. NON-AUTOREGRESSIVE DECODING SCHEME

Since the decoding scheme is another critical aspect influencing time series forecasting performance, this section is dedicated to elucidating the strengths and weaknesses of both decoding methods and discussing how we should choose between them in different data scenarios.

Autoregressive models excel with strong seasonality but struggle with pronounced trends.

Table 5 indicates that autoregressive methods generally exhibit inferior performance to non-autoregressive ones in long-term datasets. However, notable exceptions exist, autoregressive models display superior efficacy on the Traffic dataset, which is of minimal trend strength (see Table 3). Under this situation, the autoregressive methods even surpass the state-of-the-art non-autoregressive models. Detailed examination reveals the difficulties autoregressive models face in datasets with significant trends like ETT, while they fare well in modeling strong seasonality, as evident in the Electricity and Traffic datasets. This manifests the proficiency of autoregressive models in capturing seasonal patterns but their inadequacy in modeling long-term trends.

Both decoding schemes perform equally well in short-term forecasting.

Table 4 implies a comparable performance between two decoding schemes in short-term forecasting datasets. This is possibly attributed to the limited impact of error propagation on autoregressive methods in short-term scenarios. Additionally, the flexibility of the autoregressive approaches makes it a feasible choice for accommodating diverse temporal structures and complexities in short-term prediction datasets.

The experimental findings reveal that while autoregressive methods are proficient in modeling seasonality, they falter in managing long-term trends, an area where non-autoregressive methods demonstrate competency. This divergence in expertise serves as a guideline for selecting decoding schemes for particular data scenarios. It also explains the preferential biases of the aforementioned two branches towards specific decoding manner. Interestingly, there are cases where autoregressive methods outperform non-autoregressive ones in long-term situations, especially in datasets with strong seasonal patterns. This finding leads us to speculate that enhancing autoregressive models to curb error propagation and adeptly handle trending data could make them strong challengers in providing long-term forecasting solutions.

4.5 COMPUTATIONAL EFFICIENCY

The necessity to depict intricate, high-dimensional data distributions in modern applications introduces considerable computational challenges in time-series forecasting, a crucial aspect often neglected by prior research. Thus, we provide a computational efficiency analysis here.

Modeling high-dimensional probabilistic distributions demands substantial memory and is time-intensive.

In Figure 6a, a significant escalation in GPU memory consumption is observed with the increase in the number of variates, where CSDI—integrating non-autoregressive decoding schemes with a diffusion model—exhibits a particularly pronounced surge. Additionally, Figure 6b reveals that methods centered on probabilistic estimation entail longer inference times, especially the Diffusion model, which requires stepwise denoising processes. These findings underscore the crucial need for optimizing memory efficiency and reducing inference time, particularly as the prediction horizon extends.

5 CONCLUSION

In conclusion, this paper has presented `ProbTS`, a novel toolkit developed to advance the field of time-series forecasting by synergizing and comparing research branches emphasizing neural architecture designs with the one focusing on advanced probabilistic estimations. Through `ProbTS`, we have answered several pivotal research questions stemming from the divergences in data scenarios, methodologies, and decoding schemes between these distinct branches. Looking ahead, there is immense potential in amalgamating the strengths of both branches to redefine the future of time-series forecasting. We anticipate that the `ProbTS` toolkit will act as a catalyst, expediting groundbreaking research in this domain, and unlocking new possibilities for refined and robust forecasting models.

REFERENCES

- Alexander Alexandrov, Konstantinos Benidis, Michael Bohlke-Schneider, Valentin Flunkert, Jan Gasthaus, Tim Januschowski, Danielle C. Maddix, Syama Rangapuram, David Salinas, Jasper Schulz, Lorenzo Stella, Ali Caner Türkmen, and Yuyang Wang. GluonTS: Probabilistic and Neural Time Series Modeling in Python. *Journal of Machine Learning Research*, 21(116):1–6, 2020.
- Rafal A Angryk, Petrus C Martens, Berkay Aydin, Dustin Kempton, Sushant S Mahajan, Sunitha Basodi, Azim Ahmadzadeh, Xumin Cai, Soukaina Filali Boubrahimi, Shah Muhammad Hamdi, et al. Multivariate Time Series Dataset for Space Weather Data Analytics. *Scientific data*, 7(1): 227, 2020.
- Shane Bergsma, Timothy Zeyl, Javad Rahimipour Anaraki, and Lei Guo. C2FAR: Coarse-to-Fine Autoregressive Networks for Precise Probabilistic Forecasting. In *In Proc. of NeurIPS*, 2022.
- Marin Bilos, Kashif Rasul, Anderson Schneider, Yuriy Nevmyvaka, and Stephan Günnemann. Modeling Temporal Data as Continuous Functions with Stochastic Process Diffusion. In *In Proc. of ICML*, pp. 2452–2470, 2023.
- Cristian Challu, Kin G. Olivares, Boris Oreshkin, Federico Ramirez, Max Canseco, and Artur Dubrawski. NHITS: Neural Hierarchical Interpolation for Time Series Forecasting. In *In Proc. of AAAI*, pp. 6989–6997, 2023.
- Razvan-Gabriel Cirstea, Chenjuan Guo, Bin Yang, Tung Kieu, Xuanyi Dong, and Shirui Pan. Tri-former: Triangular, Variable-Specific Attentions for Long Sequence Multivariate Time Series Forecasting. In *In Proc. of IJCAI*, pp. 1994–2001, 2022.
- Emmanuel de Bézenac, Syama Sundar Rangapuram, Konstantinos Benidis, Michael Bohlke-Schneider, Richard Kurl, Lorenzo Stella, Hilaf Hasson, Patrick Gallinari, and Tim Januschowski. Normalizing Kalman Filters for Multivariate Time Series Analysis. In *In Proc. of NeurIPS*, pp. 2995–3007, 2020.
- Laurent Dinh, Jascha Sohl-Dickstein, and Samy Bengio. Density Estimation using Real NVP. In *In Proc. of ICLR*, 2017.
- Alexandre Drouin, Étienne Marcotte, and Nicolas Chapados. TACTiS: Transformer-Attentional Copulas for Time Series. In *In Proc. of ICML*, pp. 5447–5493, 2022.
- Vijay Ekambaram, Arindam Jati, Nam Nguyen, Phanwadee Sinthong, and Jayant Kalagnanam. TSMixer: Lightweight MLP-Mixer Model for Multivariate Time Series Forecasting. In *In Proc. of SIGKDD*, pp. 459–469, 2023.
- William Falcon and The PyTorch Lightning team. PyTorch Lightning, March 2019. URL <https://github.com/Lightning-AI/lightning>.
- Wei Fan, Shun Zheng, Xiaohan Yi, Wei Cao, Yanjie Fu, Jiang Bian, and Tie-Yan Liu. DEPTS: Deep Expansion Learning for Periodic Time Series Forecasting. In *In Proc. of ICLR*, 2022.
- Bidisha Ghosh, Biswajit Basu, and Margaret O’Mahony. Multivariate Short-term Traffic Flow Forecasting using Time-series Analysis. *IEEE transactions on intelligent transportation systems*, 10(2):246–254, 2009.
- Kaiming He, Xiangyu Zhang, Shaoqing Ren, and Jian Sun. Deep Residual Learning for Image Recognition. In *In Proc. of CVPR*, pp. 770–778, 2016.
- Jonathan Ho, Ajay Jain, and Pieter Abbeel. Denoising Diffusion Probabilistic Models. In *In Proc. of NeurIPS*, 2020.
- Guokun Lai, Wei-Cheng Chang, Yiming Yang, and Hanxiao Liu. Modeling Long- and Short-Term Temporal Patterns with Deep Neural Networks. In *In Proc. of SIGIR*, pp. 95–104, 2018.
- Yann LeCun, Yoshua Bengio, and Geoffrey Hinton. Deep Learning. *nature*, 2015.

- Shiyang Li, Xiaoyong Jin, Yao Xuan, Xiyong Zhou, Wenhui Chen, Yu-Xiang Wang, and Xifeng Yan. Enhancing the Locality and Breaking the Memory Bottleneck of Transformer on Time Series Forecasting. In *In Proc. of NeurIPS*, pp. 5244–5254, 2019.
- Yan Li, Xinjiang Lu, Yaqing Wang, and Dejing Dou. Generative Time Series Forecasting with Diffusion, Denoise, and Disentanglement. In *In Proc. of NeurIPS*, 2022.
- Bryan Lim and Stefan Zohren. Time-series Forecasting with Deep Learning: a Survey. *Philosophical Transactions of the Royal Society A*, 2021.
- Bryan Lim, Sercan Ö Arık, Nicolas Loeff, and Tomas Pfister. Temporal Fusion Transformers for Interpretable Multi-horizon Time Series Forecasting. *International Journal of Forecasting*, 2021.
- Minhao LIU, Ailing Zeng, Muxi Chen, Zhijian Xu, Qiuxia LAI, Lingna Ma, and Qiang Xu. SCINet: Time Series Modeling and Forecasting with Sample Convolution and Interaction. In *In Proc. of NeurIPS*, 2022.
- Shizhan Liu, Hang Yu, Cong Liao, Jianguo Li, Weiyao Lin, Alex X. Liu, and Schahram Dustdar. Pyraformer: Low-Complexity Pyramidal Attention for Long-Range Time Series Modeling and Forecasting. In *In Proc. of ICLR*, 2022.
- Markus Löning, Anthony J. Bagnall, Sajaysurya Ganesh, Viktor Kazakov, Jason Lines, and Franz J. Király. Sktime: A Unified Interface for Machine Learning with Time Series. *CoRR*, abs/1909.07872, 2019. URL <http://arxiv.org/abs/1909.07872>.
- James E Matheson and Robert L Winkler. Scoring Rules for Continuous Probability Distributions. *Management science*, 22(10):1087–1096, 1976.
- Yuqi Nie, Nam H. Nguyen, Phanwadee Sinthong, and Jayant Kalagnanam. A Time Series is Worth 64 Words: Long-term Forecasting with Transformers. In *In Proc. of ICLR*, 2023.
- Frank Nielsen. On the Jensen–Shannon symmetrization of distances relying on abstract means. *Entropy*, 21(5):485, 2019.
- Ignacio Oguiza. tsai - A State-of-the-art Deep Learning Library for Time Series and Sequential Data. Github, 2022. URL <https://github.com/timeseriesAI/tsai>.
- Boris N. Oreshkin, Dmitri Carпов, Nicolas Chapados, and Yoshua Bengio. N-BEATS: Neural basis expansion analysis for interpretable time series forecasting. In *In Proc. of ICLR*, 2020.
- George Papamakarios, Iain Murray, and Theo Pavlakou. Masked Autoregressive Flow for Density Estimation. In *In Proc. of NeurIPS*, pp. 2338–2347, 2017.
- Rial A Rajagukguk, Raden AA Ramadhan, and Hyun-Jin Lee. A Review on Deep Learning Models for Forecasting Time Series Data of Solar Irradiance and Photovoltaic Power. *Energies*, 13(24):6623, 2020.
- Syama Sundar Rangapuram, Matthias W. Seeger, Jan Gasthaus, Lorenzo Stella, Yuyang Wang, and Tim Januschowski. Deep State Space Models for Time Series Forecasting. In *In Proc. of NeurIPS*, pp. 7796–7805, 2018.
- Kashif Rasul, Calvin Seward, Ingmar Schuster, and Roland Vollgraf. Autoregressive Denoising Diffusion Models for Multivariate Probabilistic Time Series Forecasting. In *In Proc. of ICML*, pp. 8857–8868, 2021a.
- Kashif Rasul, Abdul-Saboor Sheikh, Ingmar Schuster, Urs M. Bergmann, and Roland Vollgraf. Multivariate Probabilistic Time Series Forecasting via Conditioned Normalizing Flows. In *In Proc. of ICLR*, 2021b.
- David Salinas, Michael Bohlke-Schneider, Laurent Callot, Roberto Medico, and Jan Gasthaus. High-dimensional Multivariate Forecasting with Low-rank Gaussian Copula Processes. In *In Proc. of NeurIPS*, pp. 6824–6834, 2019.

- David Salinas, Valentin Flunkert, Jan Gasthaus, and Tim Januschowski. DeepAR: Probabilistic Forecasting with Autoregressive Recurrent Networks. *International Journal of Forecasting*, 36(3):1181–1191, 2020.
- Chen-Yu Tai, Wun-Jhe Wang, and Yueh-Min Huang. Using Time-Series Generative Adversarial Networks to Synthesize Sensing Data for Pest Incidence Forecasting on Sustainable Agriculture. *Sustainability*, 15(10):7834, 2023.
- Yusuke Tashiro, Jiaming Song, Yang Song, and Stefano Ermon. CSDI: Conditional Score-based Diffusion Models for Probabilistic Time Series Imputation. In *In Proc. of NeurIPS*, pp. 24804–24816, 2021.
- Sean J Taylor and Benjamin Letham. Forecasting at Scale. *The American Statistician*, 2018.
- Ashish Vaswani, Noam Shazeer, Niki Parmar, Jakob Uszkoreit, Llion Jones, Aidan N. Gomez, Lukasz Kaiser, and Illia Polosukhin. Attention is All you Need. In *In Proc. of NeurIPS*, pp. 5998–6008, 2017.
- Xiaozhe Wang, Kate Smith, and Rob Hyndman. Characteristic-based Clustering for Time Series Data. *Data mining and knowledge Discovery*, 13:335–364, 2006.
- Ruofeng Wen, Kari Torkkola, Balakrishnan Narayanaswamy, and Dhruv Madeka. A Multi-horizon Quantile Recurrent Forecaster. *arXiv preprint arXiv:1711.11053*, 2017.
- Haixu Wu, Jiehui Xu, Jianmin Wang, and Mingsheng Long. Autoformer: Decomposition Transformers with Auto-Correlation for Long-Term Series Forecasting. In *In Proc. of NeurIPS*, pp. 22419–22430, 2021.
- Haixu Wu, Tengge Hu, Yong Liu, Hang Zhou, Jianmin Wang, and Mingsheng Long. TimesNet: Temporal 2D-Variation Modeling for General Time Series Analysis. In *In Proc. of ICLR*, 2023.
- Ailing Zeng, Muxi Chen, Lei Zhang, and Qiang Xu. Are Transformers Effective for Time Series Forecasting? In *In Proc. of AAAI*, pp. 11121–11128, 2023.
- Tianping Zhang, Yizhuo Zhang, Wei Cao, Jiang Bian, Xiaohan Yi, Shun Zheng, and Jian Li. Less is More: Fast Multivariate Time Series Forecasting with Light Sampling-Oriented MLP Structures. *arXiv preprint arXiv:2207.01186*, 2022.
- Yunhao Zhang and Junchi Yan. Crossformer: Transformer Utilizing Cross-dimension Dependency for Multivariate Time Series Forecasting. In *In Proc. of ICLR*, 2022.
- Haoyi Zhou, Shanghang Zhang, Jieqi Peng, Shuai Zhang, Jianxin Li, Hui Xiong, and Wancai Zhang. Informer: Beyond Efficient Transformer for Long Sequence Time-series Forecasting. In *In Proc. of AAAI*, pp. 11106–11115, 2021.
- Tian Zhou, Ziqing Ma, Qingsong Wen, Xue Wang, Liang Sun, and Rong Jin. Fedformer: Frequency Enhanced Decomposed Transformer for Long-term Series Forecasting. In *In Proc. of ICMLg*, pp. 27268–27286, 2022.

A QUANTIFYING THE CHARACTERISTICS OF DATASETS

Trend & Seasonality To gain deeper insights into the dataset characteristics, we conducted a quantitative evaluation of trend and seasonality for each dataset, drawing upon methodologies outlined in the work of Wang et al. (2006). In particular, we employed a time series decomposition model expressed as:

$$y_t = T_t + S_t + R_t,$$

where T_t represents the smoothed trend component, S_t signifies the seasonal component, and R_t denotes the remainder component. In order to obtain each component, we followed the STL decomposition approach⁴.

⁴<https://otexts.com/fpp2/stl.html>

In the case of strongly trended data, the variation within the seasonally adjusted data should considerably exceed that of the remainder component. Consequently, the ratio $\text{Var}(R_t)/\text{Var}(T_t + R_t)$ is expected to be relatively small. As such, the measure of trend strength can be formulated as:

$$F_T = \max\left(0, 1 - \frac{\text{Var}(R_t)}{\text{Var}(T_t + R_t)}\right).$$

The quantified trend strength, ranging from 0 to 1, characterizes the degree of trend presence. Similarly, the evaluation of seasonal intensity employs the detrended data:

$$F_S = \max\left(0, 1 - \frac{\text{Var}(R_t)}{\text{Var}(S_t + R_t)}\right).$$

A series with F_S near 0 indicates minimal seasonality, while strong seasonality is indicated by F_S approaching 1 due to the considerably smaller variance of $\text{Var}(R_t)$ in comparison to $\text{Var}(S_t + R_t)$.

Tables 6 depict the results for each dataset. Notably, the ETT datasets and the Exchange dataset manifest conspicuous trends, whereas the Electricity, Solar, and Traffic datasets showcase marked seasonality. Additionally, the Exchange dataset stands out with distinctive features. Figure 3 illustrates that with shorter prediction windows, the Exchange dataset sustains comparatively minor fluctuations, almost forming a linear trajectory. This enables effective forecasting through a straightforward batch mean approach. As the forecasting horizon extends, the dataset appears a more pronounced trend while retaining minimal seasonality.

Data Distribution To analyze the influence of data distribution on model performance, we measured the similarity between each dataset’s distribution and the Gaussian distribution. Specifically, we computed the Jensen–Shannon divergence (Nielsen, 2019) within a fixed-length sliding window for each variate. A window size of 30 was used for short-term datasets and 336 for long-term ones. The average of these calculations yielded the overall degree of conformity of each dataset to the Gaussian distribution. These results are summarized in Table 6.

Table 6: Quantitative assessment of intrinsic characteristics for each dataset. To eliminate ambiguity, we use the suffix “-S” and “-L” to denote short-term and long-term forecasting datasets, respectively. The JS Div denotes Jensen–Shannon divergence, where a lower score indicates closer approximations to a Gaussian distribution.

Dataset	Exchange-S	Solar-S	Electricity-S	Traffic-S	Wikipedia-S	ETTm1-L	ETTm2-L
Trend F_T	0.9982	0.1688	0.6443	0.2880	0.5253	0.9462	0.9770
Seasonality F_S	0.1256	0.8592	0.8323	0.6656	0.2234	0.0105	0.0612
JS Div.	0.2967	0.5004	0.3579	0.2991	0.2751	0.0833	0.1701
Dataset	ETTh1-L	ETTh2-L	Electricity-L	Traffic-L	Weather-L	Exchange-L	ILI-L
Trend F_T	0.7728	0.9412	0.6476	0.1632	0.9612	0.9978	0.5438
Seasonality F_S	0.4772	0.3608	0.8344	0.6798	0.2657	0.1349	0.6075
JS Div.	0.0719	0.1422	0.1533	0.1378	0.1727	0.1082	0.1112

Outliers Outliers are data points that are significantly distant from the rest, which pose challenges in forecasting. We quantified outlier ratios from both global and local perspectives. The global view treats the entire dataset as a Gaussian distribution and identifies Z-score normalized values more than 3 standard deviations from the mean as outliers. The local perspective assesses outliers within a sliding window, following the same criterion. For short-term datasets, a window size of 30 is employed, while for long-term forecasting datasets, the window size is set to 336. We present the ratio of outliers in Table 7 for reference. From Table 7, we find that some datasets, such as Wikipedia-S, possess a high local ratio of outliers, which can have a large impact on short-term forecasting.

Data Visualization To offer a clearer insight into the characteristics of each dataset and the influence of varying forecasting horizons, we have illustrated instances of both short-term and long-term

Table 7: Ratio of outliers (%). The suffix ”-S” denotes short-term forecasting datasets, while ”-L” signifies long-term forecasting datasets.

Dataset	Exchange-S	Solar-S	Electricity-S	Traffic-S	Wikipedia-S	ETTh1-L	ETTm2-L
Local	0.1718	0.2228	0.1333	0.6595	1.5435	0.4126	0.4231
Global	0.0871	0.0002	0.4210	1.6890	1.1758	1.1079	1.8764

Dataset	ETTh1-L	ETTh2-L	Electricity-L	Traffic-L	Weather-L	Exchange-L	ILI-L
Local	0.4937	0.4707	0.1529	1.4352	0.5106	0.2021	1.2422
Global	1.2951	2.1929	0.4134	1.5885	0.8323	0.0066	1.5735

forecasting datasets in Figure 2 and Figure 3 respectively. Figure 2 reveals that in short-term scenarios, time series are primarily governed by local variations. On the other hand, as depicted in Figure 3, datasets like Traffic, Electricity, and ETT, under extended forecasting horizons, display enhanced seasonality and trends, making these series more predictable.

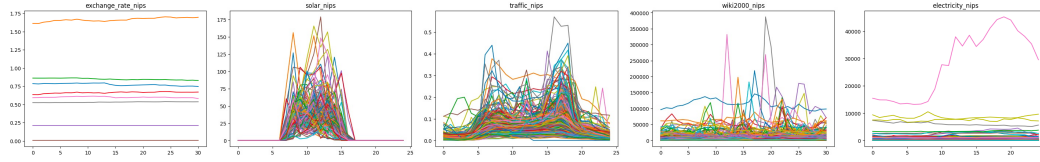


Figure 2: Time series samples extracted from the short-term forecasting dataset. The range of the x-axis is the pre-defined length of the prediction window in each dataset.

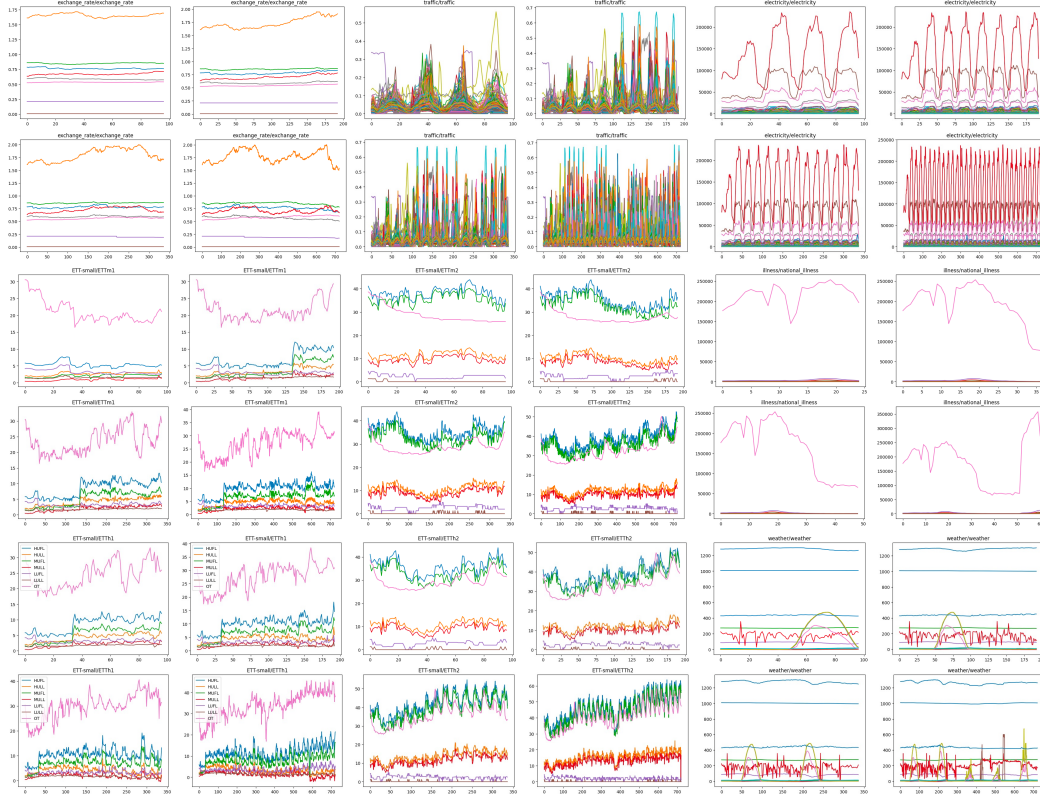


Figure 3: Time series samples extracted from the long-term forecasting dataset. The x-axis spans the pre-defined prediction window lengths within each dataset, with prediction lengths set to $T \in \{24, 36, 48, 60\}$ for the ILI dataset and $T \in \{96, 192, 336, 720\}$ for the remaining datasets.

B EVALUATION METRICS

The `ProBTS` toolkit incorporates a comprehensive range of metrics, spanning both point-level and distribution-level, to offer a nuanced and multifaceted evaluation of forecasting models.

B.1 POINT-LEVEL METRICS

For point-level metrics, we primarily focused on several measures that are predominantly used in the branch devoted to optimizing neural network architecture design.

Mean Absolute Error (MAE) The Mean Absolute Error (MAE) quantifies the average absolute deviation between the forecasts and the true values. Since it averages the absolute errors, MAE is robust to outliers. Its mathematical formula is given by:

$$\text{MAE} = \frac{1}{K \times T} \sum_{i=1}^K \sum_{t=1}^T |x_{i,t} - \hat{x}_{i,t}|,$$

where K is the number of variates, L is the length of series, $x_{i,t}$ and $\hat{x}_{i,t}$ denotes the ground-truth value and the predicted value, respectively. For multivariate time series, we also provide the aggregated version:

$$\text{MAE}_{\text{sum}} = \frac{1}{T} \sum_{t=1}^T |x_t^{\text{sum}} - \hat{x}_t^{\text{sum}}|,$$

where x_t^{sum} and \hat{x}_t^{sum} are the summation across the dimension K of $x_{i,t}$ and $\hat{x}_{i,t}$, respectively.

Normalized Mean Absolute Error (NMAE) The Normalized Mean Absolute Error (NMAE) is a normalized version of the MAE, which is dimensionless and facilitates the comparability of the error magnitude across different datasets or scales. The mathematical representation of NMAE is given by:

$$\text{NMAE} = \frac{1}{K \times T} \sum_{i=1}^K \sum_{t=1}^T \frac{|x_{i,t} - \hat{x}_{i,t}|}{|x_{i,t}|}.$$

Its aggregated version is:

$$\text{NMAE}_{\text{sum}} = \frac{1}{T} \sum_{t=1}^T \frac{|x_t^{\text{sum}} - \hat{x}_t^{\text{sum}}|}{|x_t^{\text{sum}}|}.$$

Mean Squared Error (MSE) The Mean Squared Error (MSE) is a quantitative metric used to measure the average squared difference between the observed actual value and forecasts. It is defined mathematically as follows:

$$\text{MSE} = \frac{1}{K \times T} \sum_{i=1}^K \sum_{t=1}^L (x_{i,t} - \hat{x}_{i,t})^2.$$

For multivariate time series, we also provide the aggregated version:

$$\text{MSE}_{\text{sum}} = \frac{1}{T} \sum_{t=1}^L (x_t^{\text{sum}} - \hat{x}_t^{\text{sum}})^2.$$

Normalized Root Mean Squared Error (NRMSE) The Normalized Root Mean Squared Error (NRMSE) is a normalized version of the Root Mean Squared Error (RMSE), which quantifies the average squared magnitude of the error between forecasts and observations, normalized by the expectation of the observed values. It can be formally written as:

$$\text{NRMSE} = \frac{\sqrt{\frac{1}{K \times T} \sum_{i=1}^K \sum_{t=1}^L (x_{i,t} - \hat{x}_{i,t})^2}}{\frac{1}{K \times T} \sum_{i=1}^K \sum_{t=1}^T |x_{i,t}|}.$$

For multivariate time series, we also provide the aggregated version:

$$\text{NRMSE}_{\text{sum}} = \frac{\sqrt{\frac{1}{T} \sum_{t=1}^L (x_t^{\text{sum}} - \hat{x}_t^{\text{sum}})^2}}{\frac{1}{T} \sum_{t=1}^T |x_t^{\text{sum}}|}.$$

B.2 DISTRIBUTION-LEVEL METRICS

Continuous Ranked Probability Score (CRPS) The Continuous Ranked Probability Score (CRPS) (Matheson & Winkler, 1976) quantifies the agreement between a cumulative distribution function (CDF) F and an observation x , represented as:

$$\text{CRPS} = \int_{\mathbb{R}} (F(z) - \mathbb{I}\{x \leq z\})^2 dz,$$

where $\mathbb{I}\{x \leq z\}$ denotes the indicator function, equating to one if $x \leq z$ and zero otherwise.

Being a proper scoring function, CRPS reaches its minimum when the predictive distribution F coincides with the data distribution. When using the empirical CDF of F , denoted as $\hat{F}(z) = \frac{1}{n} \sum_{i=1}^n \mathbb{I}\{X_i \leq z\}$, where n represents the number of samples $X_i \sim F$, CRPS can be precisely calculated from the simulated samples of the conditional distribution $p_{\theta}(\mathbf{x}_t | \mathbf{h}_t)$. In our practice, 100 samples are employed to estimate the empirical CDF.

For multivariate time series, the aggregate CRPS, denoted as CRPS_{sum} , is derived by summing across the K time series, both for the ground-truth data and sampled data, and subsequently averaging over the forecasting horizon. Formally, it is represented as:

$$\text{CRPS}_{\text{sum}} = \mathbb{E}_t \left[\text{CRPS} \left(\hat{F}_{\text{sum}}(t), \sum_{i=1}^K x_{i,l}^0 \right) \right].$$

C EXPERIMENTS

C.1 IMPLEMENTATION DETAILS

`PROBTS` is implemented using PyTorch Lightning (Falcon & The PyTorch Lightning team, 2019). During the training, we sample 100 batches per epoch and train for a maximum of 50 epochs, employing the CRPS metric as the monitor for checkpoint saving. We employ the Adam optimizer for all experiments, which are executed on single NVIDIA Tesla V100 GPUs using CUDA 11.3. In the evaluation phase, we sample 100 times to report the metrics on the test set.

For models where optimal hyperparameters are not provided, we conduct an extensive grid search to determine the most effective settings. All optimal hyperparameter configurations identified for each model on every dataset are documented and will be accessible via a GitHub repository, to be open-sourced subsequent to the paper’s publication.

C.2 CASE STUDY

To intuitively demonstrate the distinct characteristics of point and probabilistic estimations, a case study was conducted on short-term datasets. Figure 4 illustrates that point estimation yields single-valued, deterministic estimates, in contrast to probabilistic methods, which model continuous data distributions as depicted in Figure 5. This modeling of data distributions captures the uncertainty in forecasts, aiding decision-makers in fields such as weather and finance to make more informed choices. It is also observed that while both methods align well with ground truth values in short-term forecasting datasets, they struggle to accurately capture outliers, particularly noted in the Wikipedia dataset.

C.3 MODEL EFFICIENCY

For reference, detailed results regarding memory usage and time efficiency for five representative models on long-term forecasting datasets are provided here. Table 8 displays the computation memory of various models with a forecasting horizon set to 96. Additionally, Table 9 compares the

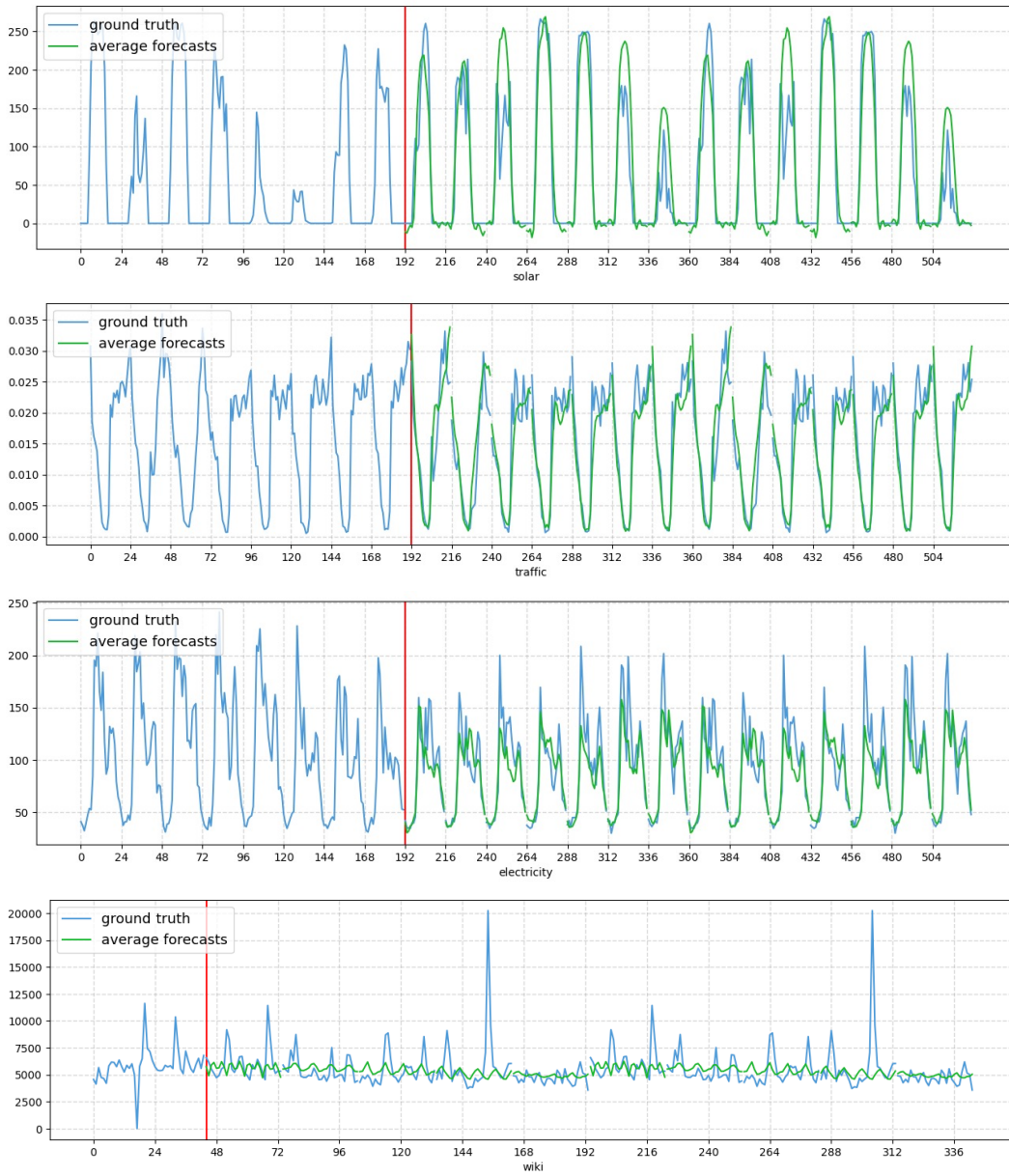


Figure 4: Point forecasts from the PatchTST model and the ground-truth value on short-term forecasting datasets.

inference time of these models on long-term forecasting datasets, illustrating the impact of changes in the forecasting horizon.

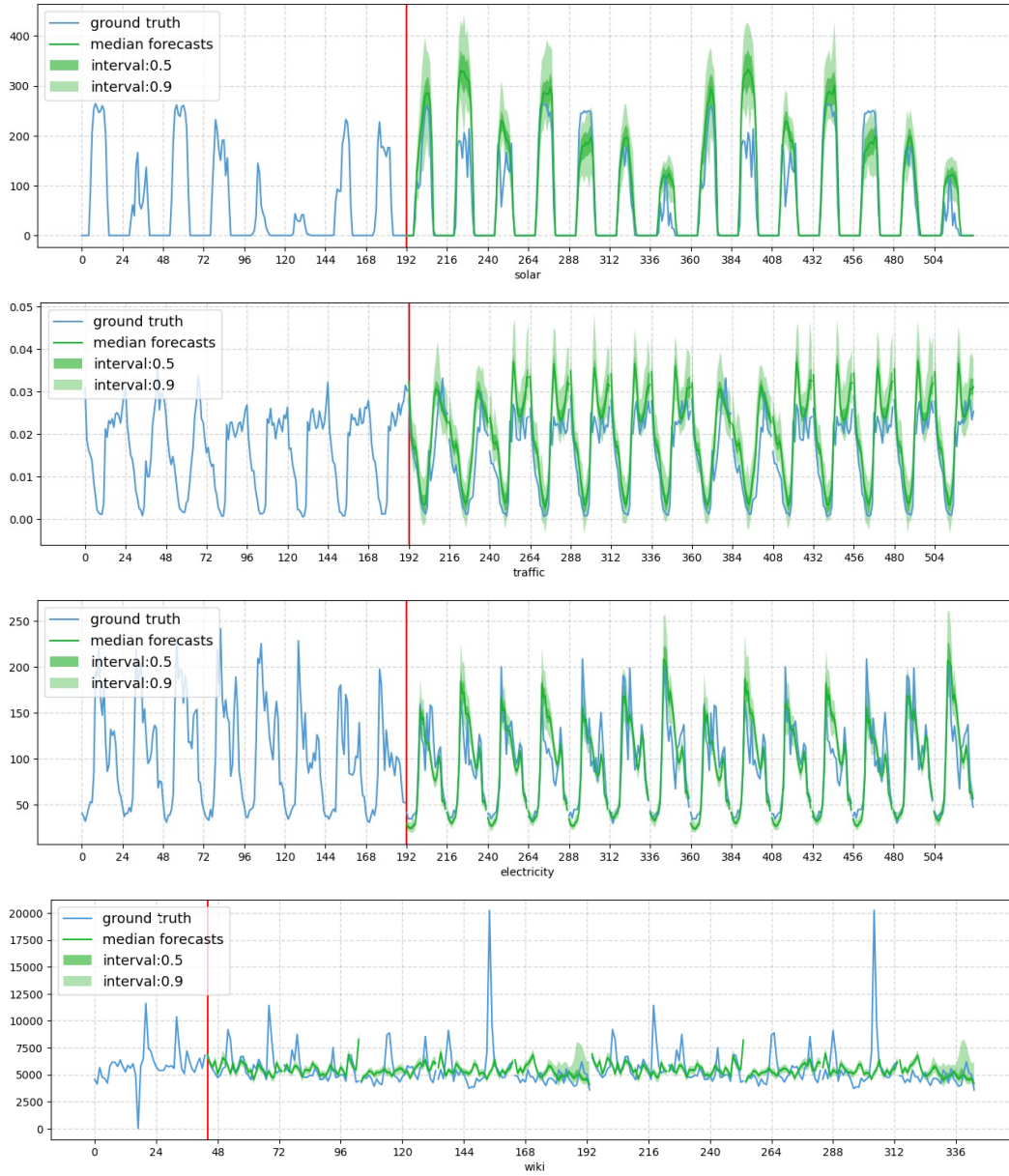


Figure 5: Forecasting intervals from the TimeGrad model and the ground-truth value on short-term forecasting datasets.

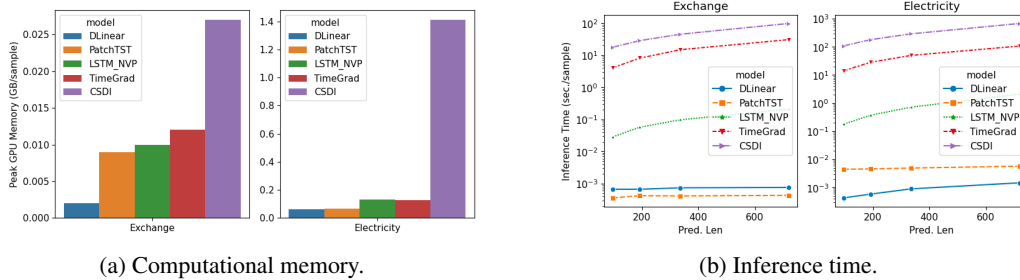


Figure 6: Comparison of computational efficiency. The forecasting horizon is set to 96 for calculating memory usage.

Table 8: Computation memory. The batch size is 1 and the prediction horizon is set to 96.

Metric	Dataset	DLinear	PatchTST	LSTM NVP	TimeGrad	CSDI
NPARAMS (MB)	ETTm1	0.075	2.145	1.079	1.233	1.720
	Electricity	0.076	2.146	3.680	3.472	1.370
	Traffic	0.078	2.149	15.926	8.298	1.390
	Weather	0.075	2.145	3.085	0.574	1.721
	Exchange	0.075	0.135	1.979	0.488	1.720
Max GPU Mem. (GB)	ETTm1	0.002	0.009	0.010	0.012	0.027
	Electricity	0.060	0.068	0.129	0.128	1.411
	Traffic	0.161	0.168	0.361	0.333	9.102
	Weather	0.004	0.012	0.021	0.012	0.070
	Exchange	0.002	0.002	0.013	0.008	0.030

Table 9: Comparison of inference time (sec./sample).

Model	pred len	DLinear	PatchTST	LSTM NVP	TimeGrad	CSDI
ETTm1	96	0.0003 ± 0.0000	0.0003 ± 0.0000	0.0352 ± 0.0007	4.1067 ± 0.0504	16.3280 ± 0.0747
	192	0.0003 ± 0.0000	0.0003 ± 0.0000	0.0697 ± 0.0020	7.8979 ± 0.0403	25.8378 ± 0.3124
	336	0.0003 ± 0.0000	0.0003 ± 0.0000	0.1221 ± 0.0044	13.6197 ± 0.1023	39.8832 ± 0.2157
	720	0.0004 ± 0.0000	0.0003 ± 0.0000	0.2603 ± 0.0020	28.6074 ± 1.1346	86.1862 ± 0.1863
Electricity	96	0.0004 ± 0.0000	0.0045 ± 0.0001	0.1783 ± 0.0006	13.8439 ± 0.0054	388.3150 ± 0.2155
	192	0.0006 ± 0.0000	0.0046 ± 0.0000	0.3700 ± 0.0010	27.6683 ± 0.0368	659.4284 ± 0.2003
	336	0.0008 ± 0.0000	0.0049 ± 0.0000	0.7157 ± 0.0028	48.4456 ± 0.0279	-
	720	0.0015 ± 0.0000	0.0057 ± 0.0000	2.0785 ± 0.0186	104.1473 ± 0.1465	-
Traffic	96	0.0010 ± 0.0001	0.0102 ± 0.0000	0.3695 ± 0.0022	31.7644 ± 0.0101	-
	192	0.0013 ± 0.0000	0.0106 ± 0.0000	0.8287 ± 0.0094	63.5832 ± 0.0060	-
	336	0.0020 ± 0.0000	0.0114 ± 0.0001	1.6945 ± 0.0026	111.4147 ± 0.0169	-
	720	0.0039 ± 0.0000	0.0137 ± 0.0000	5.0963 ± 0.0018	258.1274 ± 0.6088	-
Weather	96	0.0002 ± 0.0000	0.0004 ± 0.0000	0.0800 ± 0.0016	4.1261 ± 0.0812	37.8984 ± 0.0782
	192	0.0003 ± 0.0000	0.0004 ± 0.0000	0.1568 ± 0.0008	8.2913 ± 0.5544	62.0223 ± 0.2329
	336	0.0003 ± 0.0000	0.0004 ± 0.0000	0.2482 ± 0.0297	14.2391 ± 0.4891	96.8704 ± 0.2258
	720	0.0003 ± 0.0000	0.0005 ± 0.0000	0.5447 ± 0.0249	29.4407 ± 0.3519	216.6044 ± 0.4253
Exchange	96	0.0006 ± 0.0000	0.0004 ± 0.0000	0.0284 ± 0.0001	4.1069 ± 0.0981	17.8655 ± 0.1282
	192	0.0007 ± 0.0000	0.0004 ± 0.0000	0.0563 ± 0.0008	8.1576 ± 0.0911	28.5456 ± 0.0873
	336	0.0007 ± 0.0000	0.0004 ± 0.0000	0.0966 ± 0.0007	14.4593 ± 0.4466	44.9733 ± 0.3820
	720	0.0007 ± 0.0000	0.0004 ± 0.0000	0.2085 ± 0.0046	30.1443 ± 0.5378	97.7417 ± 0.2606
ILI	24	0.0002 ± 0.0000	0.0008 ± 0.0001	0.0080 ± 0.0001	1.0427 ± 0.0190	12.4038 ± 0.1681
	192	0.0002 ± 0.0000	0.0008 ± 0.0000	0.0121 ± 0.0003	1.5762 ± 0.0282	12.7187 ± 0.1344
	336	0.0002 ± 0.0000	0.0008 ± 0.0000	0.0155 ± 0.0002	2.1344 ± 0.0660	12.7386 ± 0.1868
	720	0.0002 ± 0.0000	0.0008 ± 0.0000	0.0196 ± 0.0004	2.5787 ± 0.0594	12.5407 ± 0.0481